THE ASTROPHYSICAL JOURNAL, 221:114–123, 1978 April 1

NONTHERMAL GALACTIC EMISSION BELOW 10 MEGAHERTZ

JAMES C. NOVACO AND LARRY W. BROWN
Infrared and Radio Astronomy Branch, Laboratory for Extraterrestrial Physics,
Goddard Space Flight Center, Greenbelt, Maryland
Received 1977 July 19; accepted 1977 September 29

ABSTRACT

The *Radio Astronomy Explorer 2* (*RAE 2*) lunar orbiting satellite has provided new measurements of the nonthermal galactic radio emission at frequencies below 10 MHz. Measurements of the emission spectra are presented for the center, anticenter, north polar, and south polar directions at 22 frequencies between 0.25 and 9.18 MHz. Survey maps of the spatial distribution of the observed low-frequency galactic emission at 1.31, 2.20, 3.93, 4.70, 6.55, and 9.18 MHz are presented. The observations were obtained with the 229 m traveling-wave V antenna on this lunar orbiting spacecraft. The improved frequency coverage offers additional insights into the structure of the local galactic neighborhood.

Subject headings: galaxies: Milky Way — galaxies: structure — radio sources: extended

I. INTRODUCTION

The *Radio Astronomy Explorer 2* (*RAE 2*) satellite is the second in a series launched for the exclusive purpose of making low-frequency astronomical measurements of the planets, of the Sun, and of our Galaxy. In this paper, investigations of the nonthermal galactic radiation with data from *RAE 2* are presented. Among the major unexpected results from the *RAE 1* satellite were the very common and often extremely intense nonthermal radio emissions from the Earth (Herman, Caruso, and Stone 1973). Although these emissions are of great interest in themselves, they seriously interfered with attempts to measure the nonthermal galactic radiation. Therefore, the *RAE 2* was modified to be operated in lunar orbit instead of in Earth orbit like *RAE 1*. The increased distance from the Earth would not only significantly reduce the contamination caused by the terrestrial emissions, but also the resulting lunar occultations of the Earth would completely eliminate the emissions over a portion of the observing time. Improvements were made to the receiver systems to take advantage of the new environment and to utilize the experience gained from the performance of the *RAE 1* instruments.

The *RAE 2*, launched on 1973 June 10, was placed into a 1100 km circular lunar orbit 5 days later. The orbit has a period of 222 minutes and an inclination of 59° to the lunar equator. Sky coverage is obtained through a combination of orbital scans and precession of the orbital plane of −0.°14 per day along the lunar equator. This results in a precession of approximately 4 hours in right ascension and 15° in declination per year. The satellite is shielded from the terrestrial kilometric radiation by lunar occultations of the Earth which occur over a 7 day period and repeat every 2 weeks. The duration of the occultations is variable, reaching a maximum which may be up to 20% for the orbital period. At other times, the measurements of the galactic radiation are still limited somewhat by contaminating signals.

II. INSTRUMENTATION

The *RAE 2* spacecraft is a low-frequency radio astronomy observatory. A complete description of the spacecraft is given by Alexander *et al.* (1975). The antenna systems consist of two traveling-wave V antennas deployed from the spacecraft to form an X configuration, separated by a 37 m dipole antenna deployed along the minor axis of symmetry. Gravity gradient forces are used to stabilize the spacecraft so that one V antenna always points toward the lunar surface and the other points outward. This outward-directed antenna is used to scan the celestial sphere and make measurements of the galactic radiation. The antenna is 229 m in length, with an equivalent apex angle of 35°. The radiation properties of this antenna, which have been calculated by Sayre (1974), are such that the solid angle of the main lobe varies from 1 sr near 10 MHz, to approximately hemispheric near 1 MHz, to nearly dipolar at the lowest frequencies (Table 1, cols. [2] and [3]). Measurements of the radiation pattern made by scanning the Sun and Earth have confirmed this theoretical work.

The receiving system on the *RAE 2* is similar to that used on *RAE 1* (Weber, Alexander, and Stone 1971). Two types of radiometers are used to measure the galactic radiation. The first type, using the Ryle-Vonberg (RV) feedback concept, provides measurements which are insensitive to gain and bandwidth changes, and thus gives stability over the many months required to map the galactic radiation. The RV radiometer operates at nine discrete frequencies (Table 1) from 0.450 to 9.18 MHz in a sequence which requires 138 s to complete. It has an effective bandwidth of 40 kHz and a postdetection time constant of 0.1 s. A coarse output channel is obtained from the integrated

TABLE 1

OBSERVATION SUMMARY OF ERRORS

	BR Receiver					RV Receiver		
Freq. (MHz) (1)	Half-Power Points E-Plane (2)	H-Plane (3)	Relative Error (4)	IMP-6 Error (5)	Total Error (6)	Relative Error (7)	IMP-6 Error (8)	Total Error (9)
9.18	39°	61°	15%	12%	19%	16%	12%	20%*
6.55	27	55	13	12	18	8	12	15*
4.70	70	80	13	12	18	8	12	15*
3.93	53	63	10	12	16	8	12	15*
^2.80	97	84	10	12	16			
^2.20	125	93	14	12	18	7	12	14*
1.85	140	105	14	11	18			
^1.45	160	115	16	11	19			
1.31	175†	120†				6	11	13*
^1.27	180	125	14	11	18			
1.03	210	140	14	10	17			
0.900	215†	145†				8	11	14
0.870	220	150	13	10	16			
^0.737	235†	155†	19	11	22			
0.700	240†	155†				8	12	15
0.600	250†	155†	19	13	23			
0.475	265†	160†	23	14	27			
0.450	270†	160†				17	14	22
0.425	275†	160†	14	14	20			
^0.360	285†	165†	20	21	29			
0.292	295†	170†	18	26	32			
0.250	300†	170†	33	36	49			

^Frequencies near antenna resonance

*Receiver and frequency used in galactic maps.

†Estimated values

servo-loop error signal, and a fine output channel is obtained from the more accurate measurement of the noise-source output required to match the antenna signal. The time constant of the fine channel is 0.5 s. Employment of the fine output channel in the analysis of the galactic radiation for the *RAE 2* data resulted in an improvement over the *RAE 1* data where only the coarse output channel was available.

The second type of radiometer is a total-power receiver covering the frequency range 0.025–13.1 MHz in 32 discrete steps, of which 18 have been used in the measurement of the galactic radiation (Table 1). A complete cycle through the 32 steps requires 8 s. This burst receiver (BR) radiometer has an effective bandwidth of 20 kHz and a postdetection time constant of 6 milliseconds.

The receiving system was calibrated in the laboratory with improved techniques similar to those employed for the *RAE 1* (Weber *et al.*) and for the *Interplanetary Monitoring Platform 6* (*IMP 6*) spacecraft (Brown 1973). Flight data have indicated good receiver performance, with gain variations not exceeding 10% per year.

III. DATA REDUCTION

The principal problem associated with the measurements of the nonthermal galactic radiation is the contamination of the data due to emissions from the Earth, Sun, and other sources such as Jupiter and Saturn (Brown 1974*a*, *b*, 1975). This emission is primarily sporadic and will be superposed on the steady underlying signal. The assumption is made that the minimum emission observed during quiet periods is the nonthermal galactic radiation. The validity of this assumption is supported by observing those lunar occultation periods when the major sources of contamination are shielded. A second problem arises from changes in instrument performance, especially in terms of long-term drifts due to aging of the receivers. Data-handling procedures followed those developed by Alexander and Novaco (1974).

The problem of editing data to remove the contaminating sources was approached in several steps. Since the Earth is the dominant emission source, the data were examined for quiet periods free from Earth radiation. Most of the Earth's emission, particularly that above 1 MHz, occurs when the Moon, at full phase, is above the nighttime ionosphere and man-made and natural radio noise can penetrate to the spacecraft (Herman *et al.*; Alexander *et al.* 1975; Gurnett 1974; Alexander and Kaiser 1976). To eliminate most of the Earth emission, only the 12 day time period centered on the new-Moon phase was used. The data were rejected from the new-Moon periods, if a visual examination showed evidence of solar activity or additional Earth radiation.

Even with the elimination of these data, the data base still contained more than enough observations to provide extremely reliable measurements. Spectra for four cardinal directions (north galactic pole, south galactic pole, center, and anticenter) of the Galaxy were obtained from 10 new-Moon periods, or about 120 days of observation. Contour maps of the observed parts of the Galaxy were constructed from these data and an additional 224 days of data.

During the periods when the *RAE 2* was shadowed from the Sun by the lunar disk, thermal gradients caused large antenna boom-tip motions relative to the spacecraft body. This motion creates changes in the antenna impedance that appear as a 50 minute oscillation in the observed data, particularly at frequencies near the antenna resonances. None of these data was used in the spectral data analysis; however, it was necessary to use some of the less affected data to provide continuous coverage in the galactic mapping. Careful comparison with nearby data groups not affected by the thermal problems showed that the data were entirely consistent with those obtained outside this period. The standard deviation was less than 4% higher for the accepted shadow data than for the unaffected portions of the map.

Since the remaining interference is characterized by individual bursts of emission for short time intervals, these sources could be removed from the data statistically.

First, the average galactic radiation level was estimated by visual examination over 4 day periods. Then, an initial amplitude filter eliminated any observed antenna temperature more than ± 2 dB above this average level. The width of this filter was chosen by examining the maximum contrast observed on *RAE 1* and ground-based low-frequency surveys that were smoothed to the resolution of the antenna. The average was further refined, as the background measurement improved, through an iterative process. Usually no significant changes were produced after two iterations.

Because of the slow scan rate and low resolution, galactic features produce a slow variation in the observed signal as opposed to abrupt onsets of the contaminating emissions. The average signal levels in adjacent 10 minute intervals were compared; the latter interval was removed from the data base, if the average exceeded a 1.5 dB shift from the former. This had the effect of removing the solar and terrestrial bursts—particularly the onset or decay—missed with the initial filtering, as well as the telemetry anomalies which occasionally occur.

Data passing through these filters were sorted by position into $5° \times 5°$ bins of galactic longitude and latitude. As measurements were added, the average antenna temperature and its standard deviation were calculated for each bin. Data points falling more than 4 standard deviations (4σ) from the average were deleted, and the statistics recomputed. This process was repeated until all the data retained were within the 4σ range. If the number of data points in any bin fell below 10 without convergence, the data were eliminated from the analysis. After merging all the 4 day groups, the final contours of the galactic maps were constructed.

The merged data cover a time span of $2\frac{3}{4}$ years. Although it was shown that there were no short-term receiver problems, long-term drifts over this period of time had to be removed from the data by normalizing the average emission for each 4 day group to the orbital average before merging with other groups. It was shown by Alexander and Novaco (1974) with *RAE 1* data that, at these low frequencies and with such large antenna patterns, the average galactic emission does not significantly vary over an orbit of the spacecraft, regardless of the orientation of the antenna. While this prevented any direct determination of the absolute observed galactic fluxes, the difficulty in computing the absolute power received by the V antenna required an indirect method. The absolute fluxes were calculated by comparing the normalized averages to the average galactic emission observed by the *IMP 6* spacecraft (Brown 1973) and extrapolated above 2.6 MHz. The *IMP 6* spectra were obtained with a short dipole antenna whose properties were well understood. The spectra represent a reliable calibration of the average absolute flux emitted by the Galaxy and should provide a standard for the *RAE 2* normalized spectra.

The resultant spectra of the four cardinal directions—center, anticenter, north polar, and south polar galactic regions—are presented in Figures 1 and 2. The error bars shown are representative of the 1–4 MHz frequency range. The galactic maps for the frequencies 9.18, 6.55, 4.70, 3.93, 2.20, and 1.31 MHz are shown in Figures 3–8, respectively. The contours are given in units of absolute brightness temperature, as determined from comparison of the *RAE 2* average temperature with the galactic spectrum measured by *IMP 6*.

IV. ERRORS

The measurement errors encountered in the observations can be estimated and compared with those obtained from the statistical analysis of the data. Since the average galactic emission has been normalized and then scaled with the *IMP 6* absolute calibration as the standard, the measurement errors arise only from

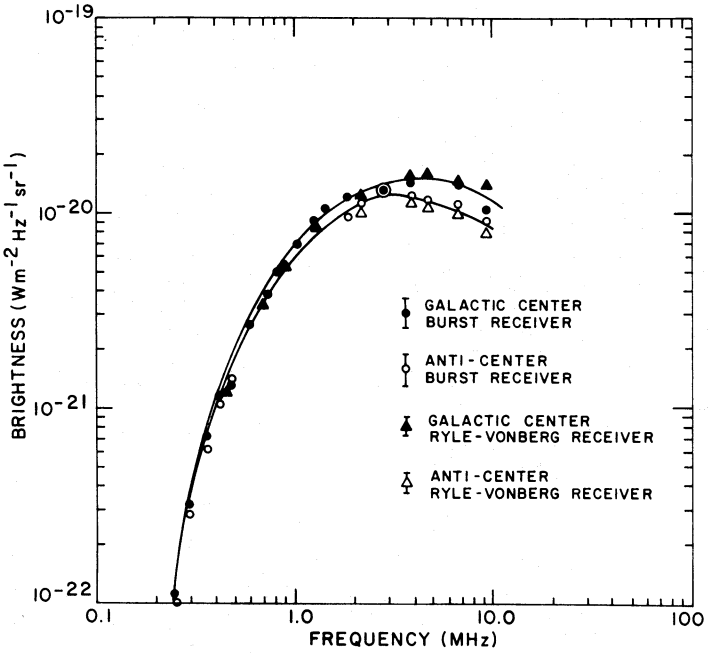

FIG. 1.—Spectra of the nonthermal emission as seen by *RAE 2* in the galactic center and anticenter directions. The error bars shown are representative of the 1–4 MHz range.

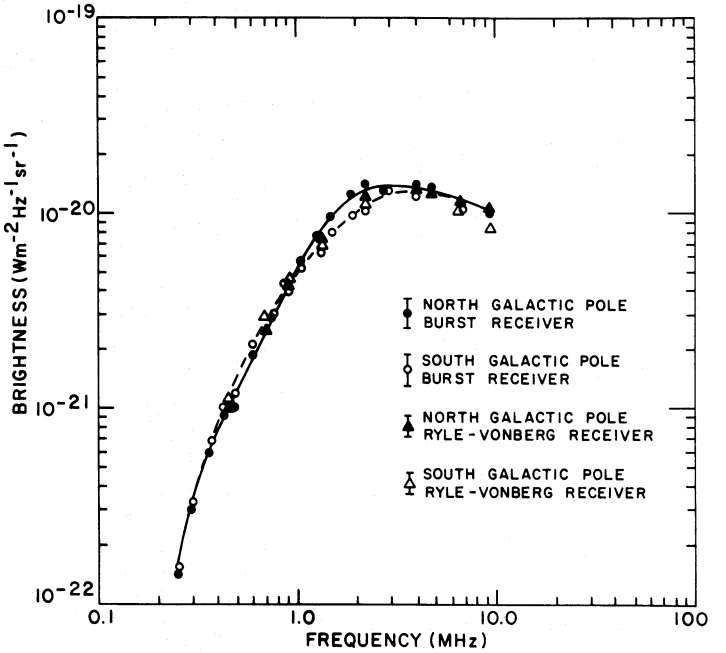

FIG. 2.—Spectra of the nonthermal emission as seen by *RAE 2* in the galactic north and south polar directions. The error bars shown are representative of the 1–4 MHz range.

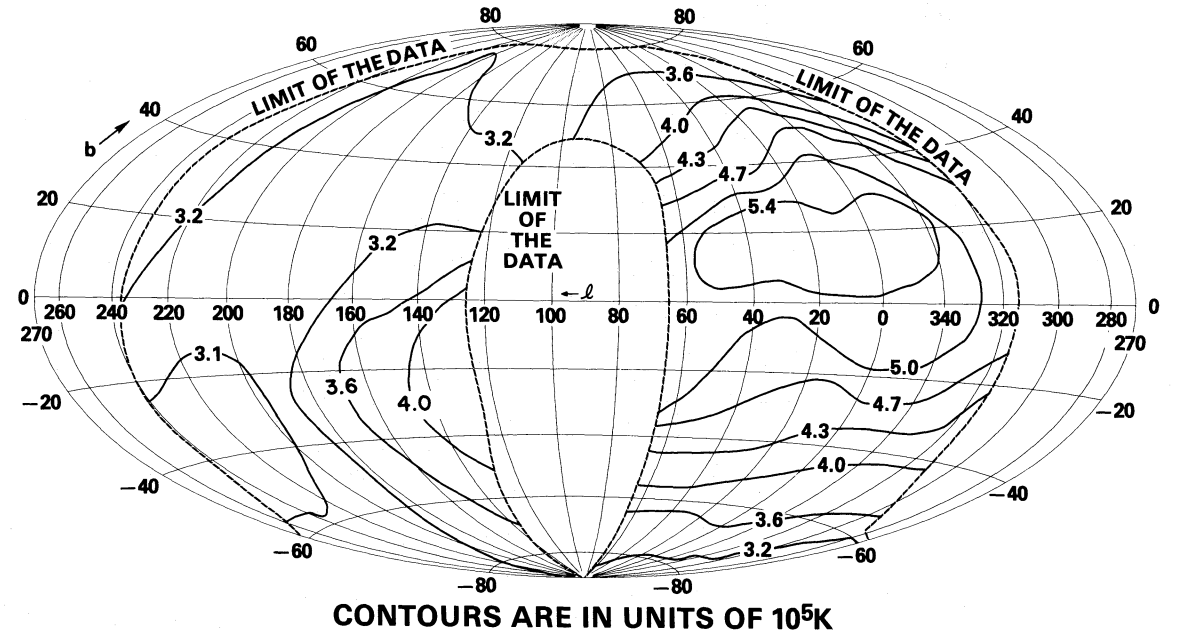

FIG. 3.—Contour map in galactic coordinates of the nonthermal emission observed by *RAE 2* at 9.18 MHz

random variations encountered in the *RAE 2* system calibration and not from any systematic trends.

The relative calibration error for the *RAE 2* system is approximately 4% for the BR receivers and 3% for the RV receivers. Other errors arise from the instabilities in the receivers. On the basis of the noise figure of the preamplifiers and the bandwidths and time constants of the system, variations of 10% for the BR receivers and 4% for the RV receivers should be expected. The short-term instability for both types of receivers appears to be less than 1%, while the long-term drift could not be corrected to better than 7%

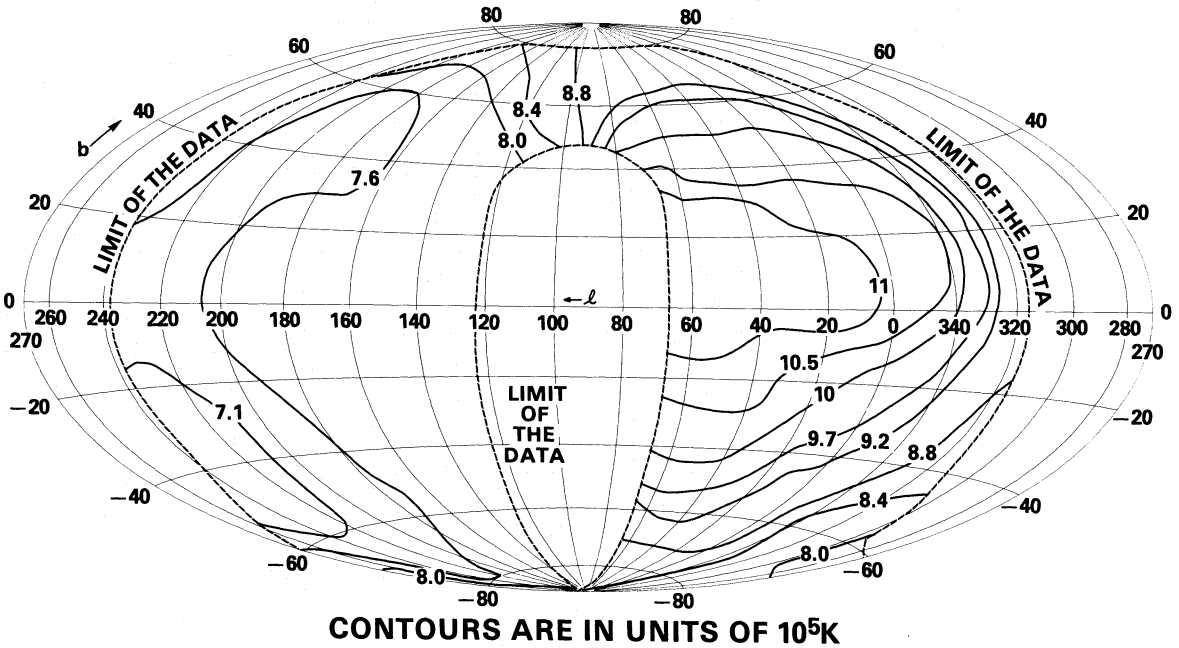

FIG. 4.—Contour map in galactic coordinates of the nonthermal emission observed by *RAE 2* at 6.55 MHz

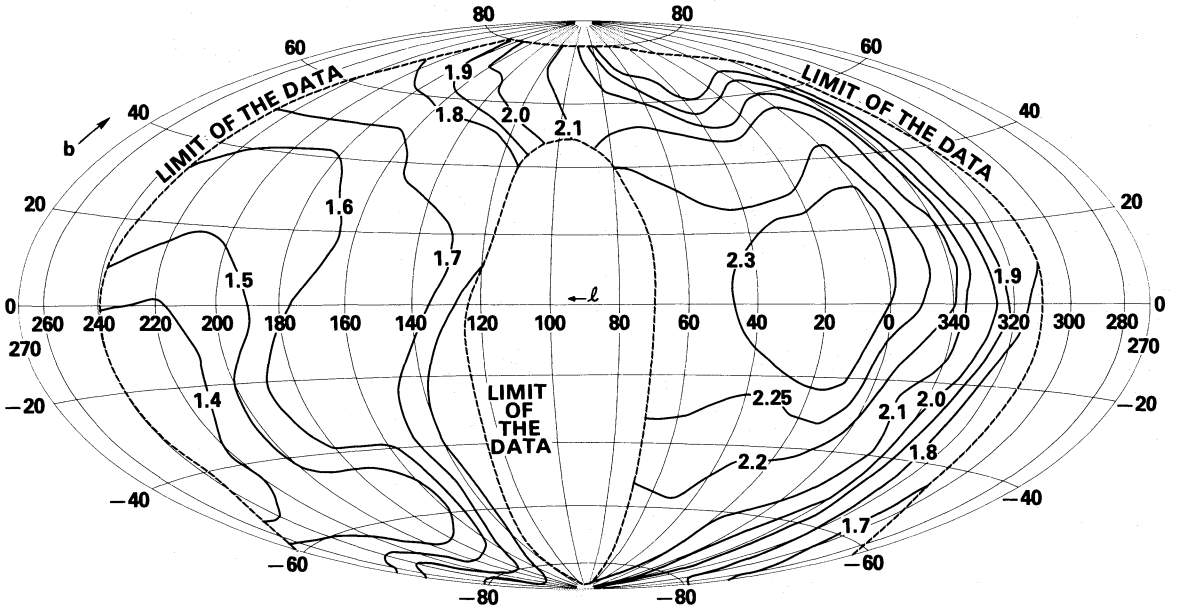

FIG. 5.—Contour map in galactic coordinates of the nonthermal emission observed by *RAE 2* at 4.70 MHz

for both. The total relative instrumental error is estimated, then, to be 14% for the BR system and 9% for the RV system.

Table 1 lists the observational errors actually observed. In this table, column (1) lists the frequencies used for the two receivers. Columns (4) and (7) give the relative error derived from the analysis of the data presented here. Columns (5) and (8) give the absolute error for the average galactic emission observed by *IMP 6* (Brown 1973). Finally, columns (6) and (9) give the total error, which is the square root of the sums of the squares of the relative and absolute errors for each

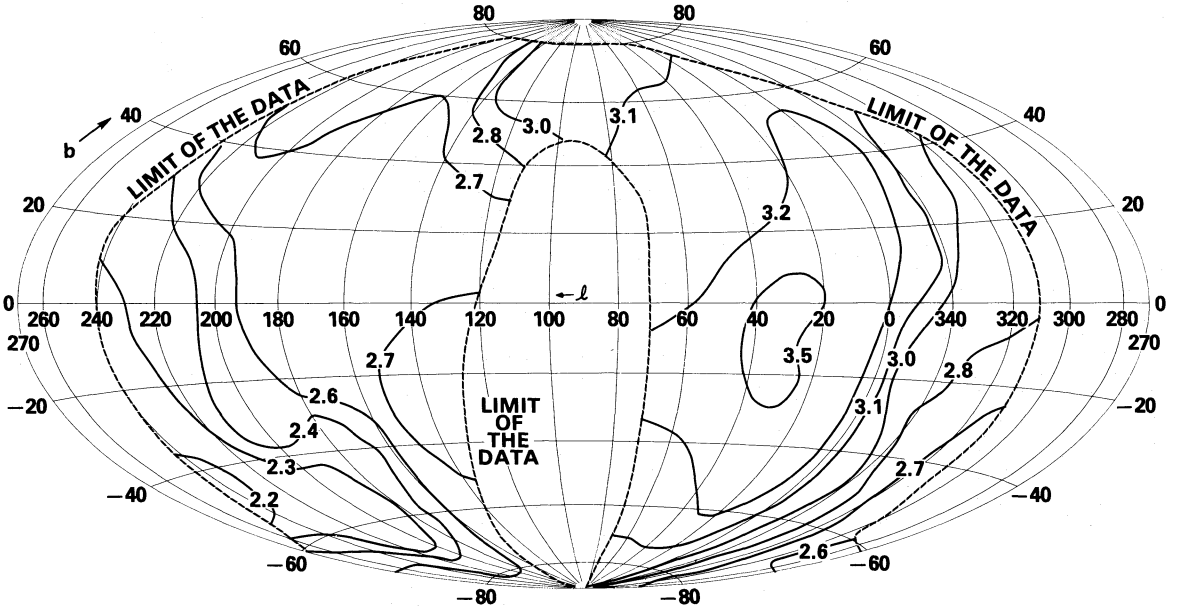

FIG. 6.—Contour map in galactic coordinates of the nonthermal emission observed by *RAE 2* at 3.93 MHz

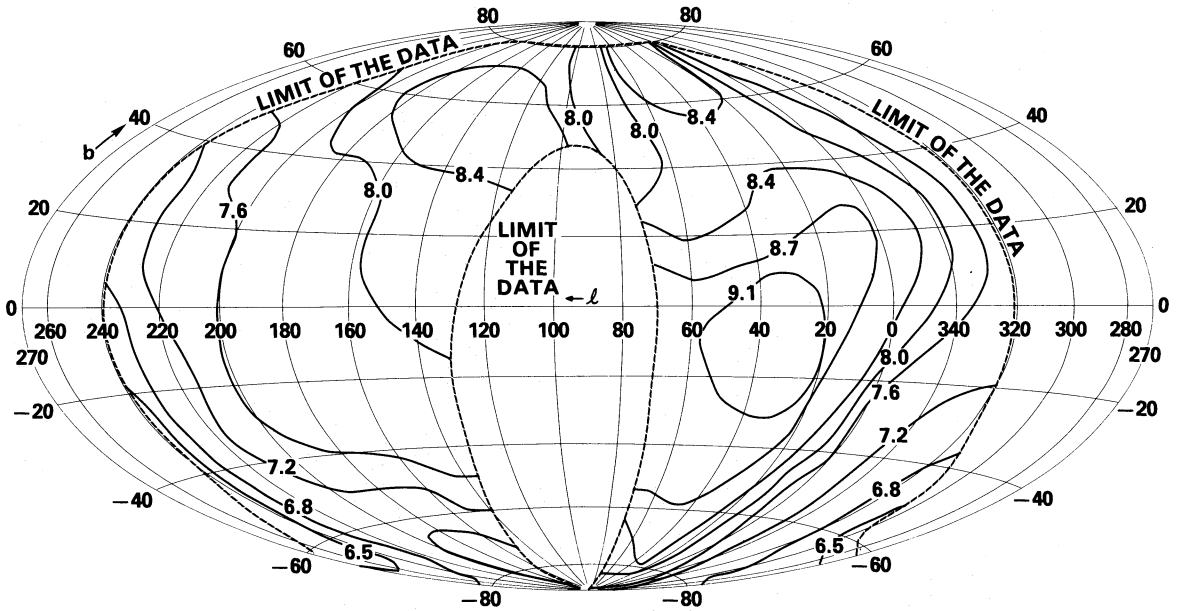

FIG. 7.—Contour map in galactic coordinates of the nonthermal emission observed by *RAE 2* at 2.20 MHz

receiver. Frequencies near antenna resonance suffer larger errors, and these are noted with a capital lambda. Those RV receiver frequencies used to produce maps of the galactic radiation are noted with an asterisk. The relative errors compare favorably with the instrumental errors, especially when the frequency dependence of the errors is taken into account.

At the time *RAE 2* was scanning the anticenter, the Sun, which was in this region of the sky, was particularly active. Even with filtering, its effect was

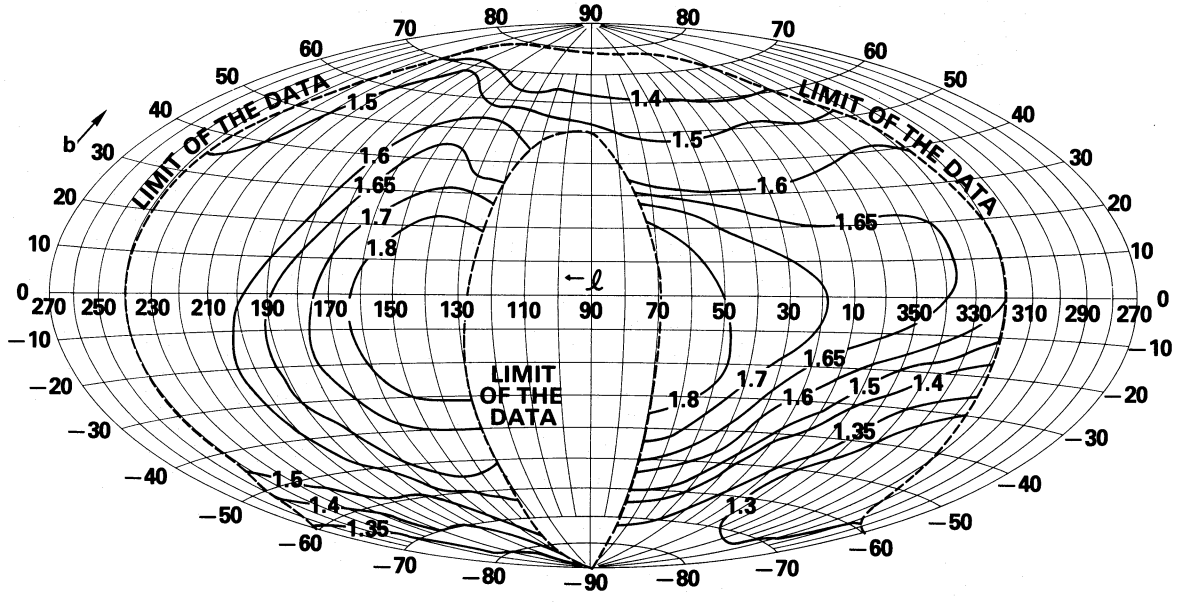

FIG. 8.—Contour map in galactic coordinates of the nonthermal emission observed by *RAE 2* at 1.31 MHz

noticeable between 0.6 and 1.5 MHz. The data above 1.5 MHz and below 0.6 MHz indicate that, in this frequency range, the spectra observed for the center and anticenter regions are probably in agreement. On the basis of this agreement, the amount of solar contamination was estimated and removed from the spectra. Naturally, the error in this portion of the spectra is somewhat larger.

In addition, some portions of the 2.2 MHz map are affected by the 50 minute oscillations resulting from solar shadowing of the antenna. At this frequency the oscillations cause an increase in the standard deviation of less than 4%.

At 9.18 MHz the data are contaminated by man-made and natural radio noise which penetrates the terrestrial ionosphere. At this end of the *RAE 2* frequency range, the ionosphere is much more transparent to electromagnetic radiation for a larger period of time. The consequence of this is the loss of a large percentage of the data, with the resulting sparsely covered map. The Penticton and Tasmanian 10 MHz surveys (Purton, Caswell, and Bridle 1970; Hamilton and Haynes 1968) were smoothed to the equivalent *RAE 2* antenna beamwidth and used to verify the manner in which the contours of the 9.18 MHz data bridged the data gaps. The resulting map is not as reliable as the other maps presented, but the increase in the error should be less than 20%.

V. DISCUSSION

At these low frequencies, the galactic radiation is composed of synchrotron emission from cosmic-ray electrons interacting with the interstellar magnetic field. While this radiation persists throughout the Galaxy, variations exist which are associated with the strength of the magnetic field and with the concentration of cosmic-ray electrons due to spiral arms, supernova remnants, and other irregularities. As the observing frequency is lowered, the emission that is observed is produced more by lower-energy cosmic-ray electrons and in regions of weaker magnetic field. In addition, free-free absorption by the thermal electrons in the ionized component of the interstellar medium becomes increasingly important. Even regions where the thermal electron density is quite low are efficient absorbers of this low-frequency radiation. Observing over a significant range of these low frequencies results in sampling the interstellar medium over a range of opacities.

This is well illustrated in the spectra of the galactic center and anticenter directions presented in Figure 1. At 10 MHz the spectra are dominated by the large-scale galactic structure. The central part of the Galaxy is brighter, because both the path length and the emissivity are greater in the inner parts of the Galaxy. At lower observing frequencies, free-free absorption reduces this path length difference so that the observed intensities in the two directions approach one another. The path lengths for the lowest frequencies are well within the local solar neighborhood (at 0.3 MHz, about 10–50 pc), and with the large beamwidths of the *RAE 2*, the average properties are the same in both directions.

The galactic polar regions (Fig. 2) show a different picture. At high frequencies, the path length extends beyond the galactic boundary in both directions, and the observed brightness includes emission from the extragalactic background (Clark, Brown, and Alexander 1970). Near 10 MHz the intensities of the north and south polar regions are nearly identical, showing very little difference in the average local properties above and below the galactic plane. However, between 1 and 4 MHz the south polar spectrum is slightly lower than that in the north. With a model of the local galactic region which was developed from the interpretation of the *RAE 1* data (Novaco and Vandenberg 1972), this difference could be reproduced by increasing the absorption in the cloud medium in a two-component model. The observed difference was reproduced either by decreasing the temperature by a factor of 2 or by increasing the cloud diameters by a factor of 4, which is the same as introducing 4 times as many clouds. Heiles (1975) has shown that the Sun is not located symmetrically with respect to the magnetoactive interstellar medium but is north of the line of symmetry. This increases the path length toward the south and causes the difference in the polar spectra.

At the lowest observing frequencies the intensities toward the four cardinal directions are equal. Since the path length is short and the antenna pattern is large, it would not be unrealistic for the local structure to appear isotropic.

The effect of observing frequency on the observed regions of the interstellar medium can be illustrated further by examining the contour maps of the observed emission (Figs. 3–8). The maps are characterized at most of the frequencies by a region of high observed emission that envelopes an area toward the galactic center and a region of low observed emission that extends well south of the galactic equator at a galactic longitude of approximately 240°. At the higher frequencies, the large-scale galactic structure dominates and the map contours tend to lie parallel to the galactic equator. At the lower frequencies, where the path length is more restricted, the map contours become normal to the galactic equator.

Centered at longitude 220° or greater is an extensive region of low observed brightness situated in an area where several factors contribute to the lack of emission. First, this region spans an area which shows a minimum of emission as observed in higher-frequency ground-based surveys (e.g., Purton *et al.*; Hamilton and Haynes 1968). The observations suggest that these areas contain either a lower magnetic field strength or a lower concentration of cosmic-ray electrons than other parts of the Galaxy. Either condition or combination of them could produce the observed minimum emission contours of the low-frequency *RAE 2* maps. A part of this area contains particularly large structures with high concentrations of ionized material (Sivan 1974). A great deal of this material is contained in two large features, the Gum nebula

($l \approx 265°$, $b \approx -5°$) and the I Ori association ($l \approx 205°$, $b \approx -15°$). At these low frequencies, this material is a highly efficient absorber, greatly contributing to the low brightness.

In the higher-frequency *RAE 2* maps, where the path extends deeply into the inner parts of the Galaxy, the high-emission region is a blend of radiation from the North Galactic Spur and the inner galactic regions. At the highest frequencies the radiation from the inner parts of the Galaxy is the dominant source shaping the contours of the maximum observed emission. The maps at lower frequencies show this area moving toward galactic longitudes nearer 40°. This is a result of a smaller contribution from the inner galactic regions due to shorter path lengths and an increasing prominence of the Spur, particularly where the Spur crosses the galactic plane. As the frequency is decreased, the nonthermal radiation becomes more absorbed by ionized material, and more distant parts of the Galaxy will contribute little, if any, to the total observed radiation; hence the Spur will be a dominant feature of the maps at these frequencies.

The 6.55 and 3.93 MHz maps (Figs. 4 and 6) agree well with those of *RAE 1* (Alexander and Novaco 1974) where the *RAE 1* data are reliable. The average brightness measured at the south galactic pole is the same for each survey, although the *RAE 2* maps indicate a gradient across the region. The high-brightness region at longitudes 20°–60° exists in both surveys but is more extended, with a slightly different centroid in the *RAE 2* maps. The low-brightness region at $l = 40°$, $b = -30°$ in the 3.93 MHz *RAE 1* maps was not reproduced by *RAE 2*; however, a featureless region at $l = 240°$, $b = -40°$ appears as a low-brightness region in the *RAE 2* maps. These discrepancies occur in regions of the sky where the *RAE 2* data are much more reliable than the *RAE 1* data.

The 4.7 MHz map contains a small area in common with the ground-based surveys of Ellis and Hamilton (1966). The agreement between the surveys is excellent, if their survey is convolved with the *RAE 2* antenna pattern; however, the gradient observed across the south galactic pole is not present in their survey. The intensity scales of the surveys agree to within a factor of 2. This is excellent agreement, given the uncertainties in the effective collecting area and solid angle of the V antenna of *RAE 2*.

At 2.20 MHz the center of maximum emission lies south of the plane at longitude ~40°. The Cetus Arc, another galactic loop, has a strong observed emission ridge in this area ($l \approx 45°$, $b \approx -40°$) and influences the location of the observed maximum by blending with the North Galactic Spur. This supposition is supported by the movement with decreasing frequency of the observed maximum away from the direction of the galactic center to ever increasing longitude as well as in a direction south of the plane. This could imply that the emission from the Cetus Arc is a more dominant feature at a lower observing frequency than that from the North Galactic Spur.

It is intriguing to speculate on the possible implications of this observation. The simplest picture would be that the emission dominance of the Cetus Arc at a lower frequency than that for the North Galactic Spur implies that the Spur lies at a greater distance from the Sun. However, for this to be correct, the absorption properties of the interstellar medium in the directions of these loops would have to be nearly identical and the loops themselves would have to have nearly identical spectra. This observation could lead to an estimate of the path length over which the galactic emission is observed at these frequencies.

In an extensive investigation of the observational evidence on the galactic loops, Berkhuijsen, Haslam, and Salter (1971) concluded that they are supernova remnants and that several of these loops should lie within a few hundred pc of the Sun. Support for the supernova hypothesis has come from the detection of diffuse nebulosities in the North Galactic Spur and the Cetus Arc (Haslam, Kahn, and Meabum 1971; Berkhuijsen 1971) and from the detection of soft X-rays from the Spur (Bunner *et al.* 1972; Cruddace *et al.* 1976). Model calculations supported by other evidence were used by Berkhuijsen (1973) to estimate the surface brightness and distance of the loops. The center of the Spur was estimated to be 130 ± 75 pc from the Sun. The Cetus Arc was 110 ± 40 pc with the same spectral index (2.7 ± 0.2) and a slightly lower surface brightness than the Spur. In a general way, this relationship between the two loops appears to be reflected in the galactic maps of the *RAE 2* observations. However, previous attempts to construct emission models for the low-frequency galactic radiation (Clark *et al.*; Brown 1973; Novaco and Vandenberg 1972) have indicated a path length which is slightly longer than that indicated above, although still of the order of hundreds of pc. Optical polarization measurements (Mathewson and Ford 1970) tend to support the smaller path length, as the effects of the loops on the polarization of starlight are first observable for stars at distances of 50–200 pc. If the supernova origin of the loops is accepted, then the previous galactic modeling must be reconsidered.

The 2.2 MHz map contains a region bounded by longitudes 320° to 30° and latitudes +50° to −90° which is common to a 2.1 MHz ground-based survey of Reber (1968). Again, the agreement between surveys is excellent when his survey is convolved with the *RAE 2* antenna pattern. Although the high-brightness region at $l = 40°$, $b = 10°$ in the *RAE 2* map is outside the common boundaries, the contours of Reber's survey near the boundary are consistent with such a region. Similarly, the validity of the low-brightness region in the *RAE 2* data at $l \geqslant 240°$ appears to be supported by the contours near this boundary. Again, a discrepancy occurs near the south galactic pole, where the ground-based survey is nearly featureless as opposed to the gradient appearing in the *RAE 2* map. The intensity scales of the surveys agree to within a factor of 4, which is reasonable given the uncertainties in the effective collecting area and solid angle of the V antenna of *RAE 2* and the uncertainty in correcting the ionosphere at 2 MHz.

The 1.31 MHz map indicates a complete change in

the observed radiation. The center of the maximum emission area is again along the galactic plane but near a longitude of approximately 100°. That neither the Cetus Arc nor the North Galactic Spur is visible indicates that the path length is now shorter than the distances to the loops (~110 pc). Thus the radiation is confined to a very localized region well within the local spiral arm. Then, the 1.31 MHz map is a reflection of the properties of the local interstellar medium and its magnetic field in the immediate neighborhood of the Sun.

Most of the knowledge of the local galactic magnetic field comes from the measurement of Faraday rotation of linearly polarized radio sources (Wright 1973; Whiteoak 1974; Gardner, Morris, and Whiteoak 1969). Mathewson and Nicholls (1968) considered both optical and radio data, and postulated the existence of a large-scale, systematic longitudinal local field directed toward $l \approx 90°$, on which was superposed a local perturbation. The longitudinal field has been verified by a number of investigations (Wright 1973; Manchester 1974; Guélin 1974); typical results yield a longitudinal field of 2.5 microgauss directed toward $l \approx 94°$ and a large-scale fluctuating component 50% larger than the longitudinal one with a correlation length of several hundred pc.

The *RAE 2* galactic map at 1.31 MHz reflects these results. The path over which this galactic emission is observed appears to be slightly less than the correlation length of the fluctuating component of the local field. One would expect a complete change in the spatial pattern of the observed emission, if the shorter path were dominated by regions with similar magnetic properties and orientations. Although the 1.31 MHz map contains no data at $l = 94°$, the observed intensity contours about this area suggest that the center of maximum emission must fall near the direction of the longitudinal field component. The map contours seem to outline the structure of the local galactic field. Unfortunately, the *RAE 2* survey does not cover the area opposite the direction of the longitudinal field. This area should have a similar structure unless the Gum nebula and I Ori association reduce the average correlation length.

In summary, the *Radio Astronomy Explorer 2* has provided new measurements of the nonthermal galactic radiation below 10 MHz. Spectra for the directions toward the galactic center, anticenter, and north and south galactic poles have been presented and discussed. Between 1 and 4 MHz, the emission in the south polar region is less than that in the northern region. This is probably caused by the longer path lengths toward the southern region. At the lowest frequencies, all four spectra are nearly identical, which indicates that the paths are restricted to an isotropic region in the solar neighborhood.

Maps of the spatial distribution are presented at six frequencies. While the contrast in the maps is low because of the large beamwidths, the North Galactic Spur and the Cetus Arc are seen in emission and the Gum nebula and the I Ori association are seen in absorption. At 1.31 MHz the radiation path is restricted to the solar neighborhood. The only dominant feature observed is probably related to the local magnetic field.

We gratefully acknowledge our many colleagues who have helped build and operate this satellite. We thank P. Harper for her capable help in the data processing. We also acknowledge the help of Drs. W. C. Erickson, F. J. Kerr, A. J. Klimas, and R. G. Stone; Mr. J. K. Alexander; and Ms. H. Malitson for critical readings of this manuscript and helpful suggestions.

REFERENCES

Alexander, J. K., and Kaiser, M. L. 1976, *J. Geophys. Res.*, **81**, 5948.
Alexander, J. K., Kaiser, M. L., Novaco, J. C., Grena, F. R., and Weber, R. R. 1975, *Astr. Ap.*, **40**, 365.
Alexander, J. K., and Novaco, J. C. 1974, *A.J.*, **79**, 777.
Berkhuijsen, E. M. 1971, *Astr. Ap.*, **14**, 359.
———. 1973, *Astr. Ap.*, **24**, 143.
Berkhuijsen, E. M., Haslam, C. G. T., and Salter, C. J. 1971, *Astr. Ap.*, **14**, 252.
Brown, L. W. 1973, *Ap. J.*, **180**, 359.
———. 1974*a*, *Ap. J.*, **192**, 547.
———. 1974*b*, *Ap. J.* (*Letters*), **194**, L159.
———. 1975, *Ap. J.* (*Letters*), **198**, L89.
Bunner, A. N., Coleman, P. L., Kraushaar, W. L., and McCammon, O. 1972, *Ap. J.* (*Letters*), **172**, L67.
Clark, T. A., Brown, L. W., and Alexander, J. K. 1970, *Nature*, **228**, 648.
Cruddace, R. G., Friedman, H., Fritz, G., and Shulman, S. 1976, *Ap. J.*, **207**, 888.
Ellis, G. R. A., and Hamilton, P. A. 1966, *Ap. J.*, **143**, 227.
Gardner, F. F., Morris, D., and Whiteoak, J. B. 1969, *Australian J. Phys.*, **22**, 79.
Guélin, M. 1974, in *IAU Symposium No. 60, Galactic Radio Astronomy*, ed. F. J. Kerr and S. C. Simonson, III (Dordrecht: Reidel), p. 51.
Gurnett, D. A. 1974, *J. Geophys. Res.*, **79**, 4227.
Hamilton, J. R., and Haynes, R. F. 1968, *Australian J. Phys.*, **21**, 895.
Haslam, C. G. T., Kahn, F. D., and Meabum, J. 1971, *Astr. Ap.*, **12**, 388.
Heiles, C. 1975, *Ap. J.*, **204**, 379.
Herman, J. R., Caruso, J. A., and Stone, R. G. 1973, *Planet. Space Sci.*, **21**, 443.
Manchester, R. N. 1974, *Ap. J.*, **188**, 637.
Mathewson, D. S., and Ford, V. L. 1970, *Mem. R.A.S.*, **74**, 139.
Mathewson, D. S., and Nicholls, D. C. 1968, *Ap. J.* (*Letters*), **154**, L11.
Novaco, J. C., and Vandenberg, N. R. 1972, GSFC X-693-72-8.
Purton, C. R., Caswell, J. L., and Bridle, A. H. 1970, paper presented at meeting of Astr. Soc. Pacific, June.
Reber, G. 1968, *J. Franklin Inst.*, **285**, 1.
Sayre, E. P. 1974, *Final Rept., NASA NAS 5-24007* (AVSD-0144-74-CR).
Sivan, J. P. 1974, *Astr. Ap. Suppl.*, **16**, 163.
Weber, R. R., Alexander, J. A., and Stone, R. G. 1971, *Radio Sci.*, **6**, 1085.
Whiteoak, J. B. 1974, in *IAU Symposium No. 60, Galactic Radio Astronomy*, ed. F. J. Kerr and S. C. Simonson, III (Dordrecht: Reidel), p. 137.
Wright, W. E. 1973, Ph.D. thesis, California Institute of Technology.

LARRY W. BROWN and JAMES C. NOVACO: Code 693, Goddard Space Flight Center, Greenbelt, MD 20771